Electronic Supplementary Material (ESI) for New Journal of Chemistry.

Evaluation of ZnO-NiO/rGO hybrid electrocatalyst for enhanced oxygen reduction reaction (ORR) applications

S. Nagarani [a,b*], Jih-Hsing Chang [a*], M. Yuvaraj [c], K. Mohanraj [a], G. Dipsikha [d] and S. Balachandran[e]

[a] *Department of Environmental Engineering and Management, Chaoyang University of Technology, Taichung City, 413310, Taiwan.*

[b] *Department of Physics, Chennai Institute of Technology, Chennai, Tamil Nadu, 600069, India.*

[c] *Department of Biochemistry, SRM Arts and Science College, Kattankulathur, Chengalpettu-603203, India.*

[d] *Department of Physics, Alternative Energy Nanotechnology Laboratory, Indian Institute of Technology Madras, Chennai-600 036, India.*

[e] *Department of Physiology, Saveetha Dental College and Hospital, Saveetha Institute of Medical and Technical Science, Saveetha University, Chennai 600077, Tamil Nadu, India.*

*Corresponding author's Email: (S. Nagarani) nagaphysics89@gmail.com, (Jih-Hsing Chang) changjh@cyut.edu.tw

Material characterization

The purity and lattice parameters of the synthesized ZnO-NiO/rGO nanocomposite and bare nanoparticles were determined by recording the X-ray diffraction (XRD, Cu Ka irradiation; = 0.154) with the PAN analytical X-ray diffraction instrument. The 20°–70° 2θ range was covered by a 2 º/min scanning rate. Scanning electron microscopy (SEM, model no. MA15/EVO-18 electron microscope working at 200 V–30 KV) was used to investigate the surface morphology and energy dispersive X-ray (EDAX) of the synthesized catalysts. Transmission electron microscopy (TEM) and selected area electron diffraction pattern (SAED) images are taken with the Tecnai G^2 T20. From the JEOL 3010, high-resolution TEM (HR-TEM) images have been collected. X-ray photoelectron spectroscopy (XPS) investigations are carried out using the Omicron ESCA Probe X-ray photoelectron spectrometer. The measurements of XPS are carried out using Al Ka X-ray. The thermal stability of the catalyst materials was tested by thermogravimetric analysis (TGA). using the SDTQ600 from TA Instruments in an air environment at a rate of heating of 20 °C min-1 from ambient temperature to 1000 °C. Using the Brunauer Emmette Teller (BET) setup (JWGB Micro 122W), a specific surface area can be determined. Raman spectra were obtained using a 488 nm excitation on a HORIBA JOBIN VYON HR UV 800. The cyclic voltammetry equipment is manufactured by Sinsil International in Gujarat and Ahmedabad, India. used to determine the synthesized nanomaterials' electrochemical characteristics.

Electrochemical analysis

Electrochemical PGSTAT204-Metrohm multi Autolab (MAC90009) Potentiostat/Galvnosat was used to carry out the linear sweep voltammetry (LSV) and cyclic voltammetry (CV) examinations.

The electrocatalytic characteristics investigation employed a three-electrode setup. The rotating ring disk electrode (RRDE; the platinum ring with 6.5 mm and the outer diameter ring with 8.5 mm and 5.5 mm diameter GCE mm Pine Instrument) was used as the working electrode. The reference electrode was composed of Ag/AgCl, and the counter electrode was made of platinum. A potential range of 0.3 to 1 V vs.RHE was used for the CV measurement, which was performed in an oxygen-saturated 0.1 M KOH aqueous solution at a scan rate of 20 mV s-1. In an oxygen-saturated 0.1 M KOH aqueous solution, measurements using linear sweep voltammetry (LSV) and a rotating disk electrode (RDE) were performed. The rotation rates used were 200, 400, 800, 1200, and 1400, with a 20 mV s^{-1} scan rate from 0.3 V to 1 V. At room temperature, rotating ring-disk electrode (RRDE) measurements were taken.

Through Equations (1) and (2), all potentials are converted to the reversible hydrogen electrode (RHE).

$$E_{RHE} = E_{Ag/Agcl} + 0.0591 \times pH + E^{0}_{Ag/Agcl} \quad (1)$$

$$E_{RHE} = E_{Ag/Agcl} + 0.965 \quad (2)$$

The Koutecky–Levich (K-L) plot was plotted by using the below equations (3, 4 and 5). It is extensively used to investigate the ORR kinetics and calculate the number of electrons transferred to an oxygen molecule by the ZnO-NiO/rGO nanocomposite [1].

$$\frac{1}{i} = \frac{1}{i_k} + \frac{1}{i_l} = \frac{1}{i_k} + \frac{1}{B\omega^{1/2}} \quad (3)$$

$$i_k = \frac{i \times i_l}{i_l - i} \quad (4)$$

In the Koutecky-Levich equation, ik is the kinetic limiting current density, i is the measured current density, i_l is the diffusion limiting current density, and ω is the rotation rate (rad s^{-1}). and 'B' is the K-L slope determined from the following formula:

$$B = 0.2nFAD_{02}^{2/3}\nu^{-1/6}C^{0}\omega^{1/2} \quad (5)$$

Where *n* represent electron transfers number, 'F' is the Faraday constant (96485 C/mol), 'ν' is the kinematic viscosity of the electrolyte (0.01 cm^2/s), 'Co_2 is the saturated centration of oxygen (1.26×10^{-6} mol/lit) and Do_2' is the diffusion coefficient of the oxygen molecule in 0.1M KOH (1.93×10^{-5} cm^2s^{-1}), and "A" is geometric of the working electrode (0.175 cm^2). Calculating the catalyst's presence involves several key parameters, including the number of electrons involved in the ORR. The slope of the K-L plot might be used to determine this characteristic by showing a linear relationship between i^{-1} versus ω^{-1}.

The percentage of peroxide released and the number of electrons (n) involved in the reaction pathway were calculated from the RRDE using the following equations:

$$n = 4 \times \frac{I_D}{I_D + I_r/N} \quad (6)$$

$$\%HO_2^- = 200 \times \frac{I_r/N}{I_D + I_r/N} \quad (7)$$

Where I_D is the disc current, I_r is the ring current, and N = 0.38 is the current collection efficiency of the Pt ring. An uncomplicated reversible ferrocyanide/ferricyanide system was used to calculate the collecting efficiency (N).

Experimental results

The HR-TEM image of ZnO-NiO/rGO nanocomposites at different nanoscales is shown in Fig. S1. From the TEM images, the results showed that NiO nanoparticles fully covered the reduced graphene oxide sheet and nanorods strongly bound with each other, which leads to increased ORR activity.

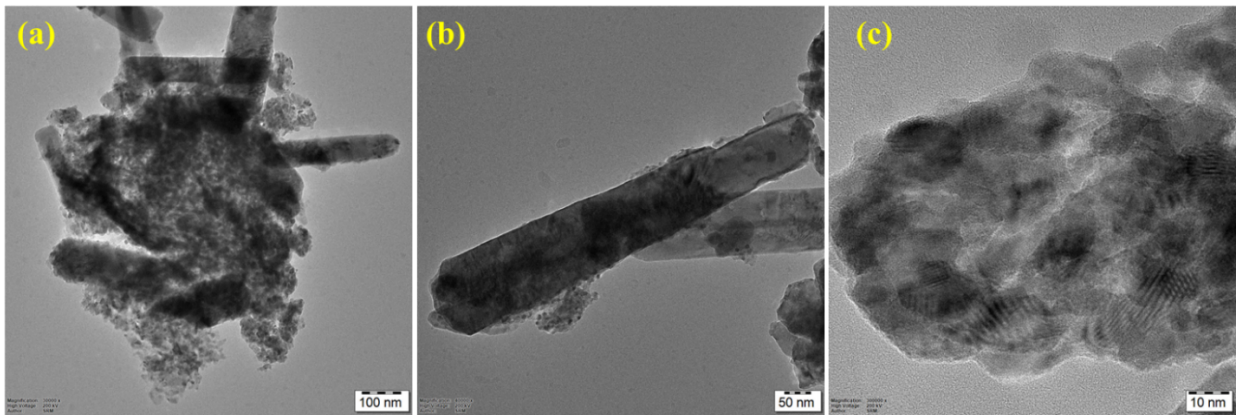

Figure. S1. (a-b) HR-TEM image of ZnO-NiO/rGO nanocomposite shows the different nanoscale.

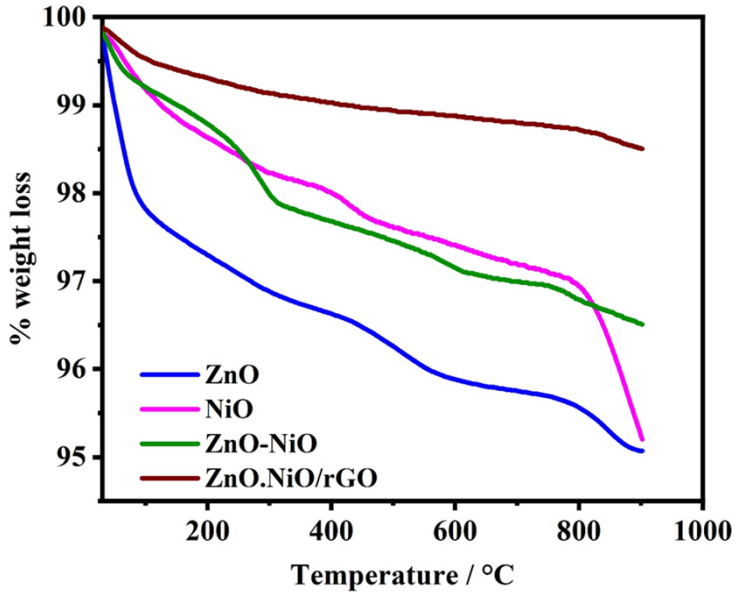

Figure. S2. TGA curves of ZnO, NiO nanoparticles, ZnO-NiO composite and ZnO-NiO/rGO nanocomposite.

Raman Spectral Analysis

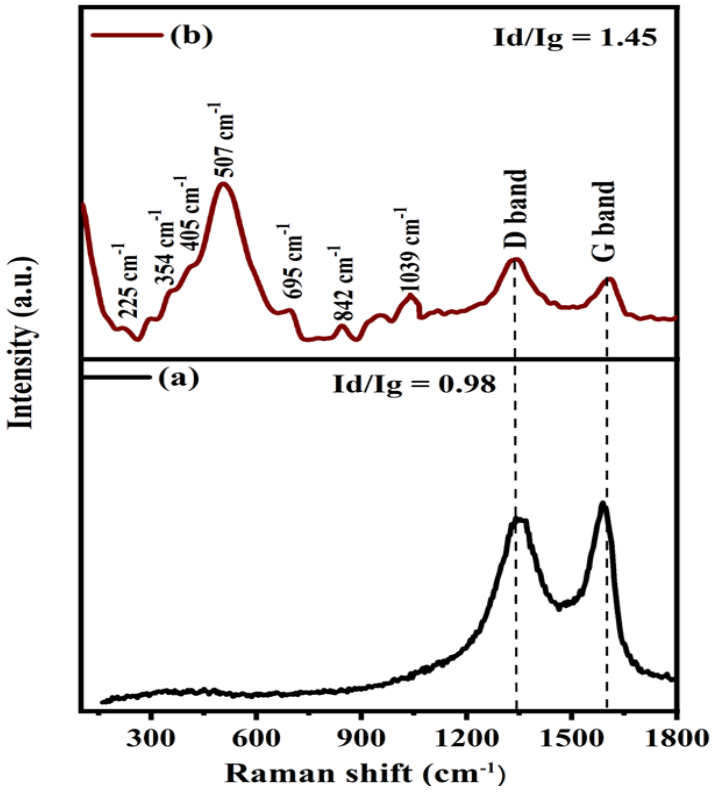

Figure. S3. Raman Spectra of synthesized nanomaterials (a) GO, (b) ZnO-NiO/rGO nanocomposite.

The synthesized nanomaterials were subjected to Raman spectra analysis, in order to further study the defects and disorder of carbon in the nanocomposite. Fig.S3 shows the Raman spectra of GO and ZnO-NiO/rGO nanocomposite. Fig. S3(a) represents Raman spectra of GO sheets functional group vibration. The peak intensity of the GO sheet shows increased intensity with both D and G bands. Fig. S3 (b) represents the vibration spectra of ZnO-NiO/rGO nanocomposite. From the obtained spectra it was observed that there was a presence of two broad characteristic peaks 1339 cm^{-1} and1598 cm^{-1} that represented the presence of D and G band respectively. The obtained D and G band represent the first ordered scattering of E_{1g} vibration

mode of sp^2 bonded carbon atoms and breathing mode of A_{1g} symmetry vibration. The intensity of I_D/I_G ratio for GO and ZnO-NiO/rGO nanocomposite has been found to be increased from 0.98 to 1.45 respectively, that indicated the presence of more defects in the rGO. For the Raman spectrum of ZnO-NiO/rGO composite, except the G band and D band, a characteristic Raman peak of ZnO nanoparticles was observed at 225, 344, 405 cm^{-1} which correspond to optical phonon of A1 mode of ZnO nanorod. The broad peaks at 507 cm^{-1} observed in the Raman spectra are corresponding to Ni-O stretching vibration of NiO that has also appeared in the composite materials [2]. The results discussed below revealed the nanocomposite formation of ZnO-NiO with reduced graphene oxide with much higher electrocatalytic activity towards ORR than its bare metal oxides nanoparticles and ZnO-NiO composite. The synergistic effect of ZnO-NiO/rGO nanocomposite materials may lead to superior electrochemical performance.

Table S1: Different Electrocatalysts' ORR Performances in 0.1 M KOH Solution Saturated with O_2.

Catalyst	**Current density (mA cm^{-2})**	**onset potential (V vs RHE)**	**Stability (current retention)**	**Reference**
ZnO-NiO/rGO hybrid	**4.2**	**0.95**	**98 % (24 h)**	**This work**
ZnO/rGO	9.21	-0.22V	92 % (4.4)	[3]
$NiCo_2O_4$	3.42	0.91	-	[4]
Mn-ZnO	-6.0	0.90	53 % (5 h)	[5]
$Cu_{0.3}Ni_{0.6}$/rGO	2.08	0.8 V	92 % (4.4 h)	[6]
$NiCoMnO_2$/N-rGO	14.2	0.92	91 % (4.5 h)	[7]
CuO.NiO/rGO	2.9	0.8	53 % (5 h)	[8]
$NiCo_2O_4$–NiO-rGO	0.84	0.92	-	[9]
ZnO@rGO	-6.0	0.90	94 % (4 h)	[10]
CuO/ZnO/NC-600	9.2	0.91	90 % (24 h)	[9]

Reference

1. P. Gokuladeepan, and A. Karthigeyan, *Appl. Surf. Sci,*2018, 449, 705-711.
2. N. Mironova-Ulmane, A. Kuzmin, J. Grabis, I. Sildos, V. I. Voronin, I.F. Berger, and V.A Kazantsev, *Solid State Phenom*, 2011, 341, 168-169.
3. J. Yu, T. Huang, Z. Jiang, M. Sun, and C. Tang, *Molecules*, 2018, 23, 3227.
4. J. Bejar, L. Alvarez-Contreras, J. Ledesma-Garcia, N. Arjona, and L.G. Arriaga, *J. Electroanal. Chem*, 2019, 847,113190.
5. M.R. Shakil, A.M. El-Sawy, H. Tasnim, A.G. Meguerdichian, J. Jin, J.P. Dubrosky, and S.L. Suib, *Inorg.Chem*, 2018, 57, 9977-9987.
6. J. Yu, Z. Jiang, J. Wang, H. Fang, T. Huang, and S. Sun, *Int. J. Hydrog. Energy*, 2019, 26, 13345-13353.
7. A. Pendashteha, J. Palma, M. Anderson, and R. Marcillaa, *Appl. Catal. B: Environ*, 2017, 201, 241–252.
8. S. Nagarani, G. Sasikala, M. Yuvaraj, G. Dipsikha, K. Mohanraj, R. Kothandaraman, and S. Balachandran, *Environ. Sci.* 2022, 211 (112992.
9. L. Preda, N. Spataru, J. M.C. Moreno, S. Somacescu, M. Marcu, *Electrocatalysis*. 2020, 11, 443–453.
10. Y. Shuo, H. Taizhong, R. Haider, F. Hengyi, Y. Jiemei, J. Zhankun, L. Dong, S. Yue, and Y. Xianxia, *Electrochemistry*, 2020, 26, 270-280.
11. D. Mahato, T. Gurusamy, S.K. Jain, K. Ramanujam, P. Haridoss, and T. Thomas, *Mater. Today. Chem*, 2022, 26, 101167.